

Relationship of structural disorder and stability of supercooled liquid state with glass-forming ability of metallic glasses

J.B. Cui^{a,*}, R.A. Konchakov^b, G.V. Afonin^b, A.S. Makarov^b, G.J. Lyu^a, J.C. Qiao^a, N.P. Kobelev^c, V.A. Khonik^b

^a*School of Mechanics, Civil Engineering and Architecture, Northwestern Polytechnical University, Xi'an 710072, China*

^b*Department of General Physics, Voronezh State Pedagogical University, Lenin St. 86, Voronezh 394043, Russia*

^c*Institute of Solid State Physics RAS, Chernogolovka, 142432, Russia*

Abstract

We performed calorimetric studies of 26 metallic glasses and calculated the excess entropy and excess enthalpy with respect to their counterpart crystals. On this basis, we introduced a dimensionless entropy-based parameter σ_{scl} , which characterizes structural disordering and stability of the supercooled liquid state upon heating. A very good correlation of σ_{scl} with literature data on the critical cooling rate R_c and critical diameter D_{max} of metallic glasses is shown. We also introduced another dimensionless parameter η_{scl} based on the excess enthalpy of glass and showed that η_{scl} provides equally good correlation with R_c and D_{max} . Possible relationship of structural disordering and glass-forming ability in the supercooled liquid range with the defect structure of glass is discussed. The obtained results provide a new window for the understanding of the glass-forming ability of metallic glasses.

Keywords: metallic glasses, excess entropy, excess enthalpy, disordering, critical cooling rate, critical diameter, defects

1. Introduction

Melts of different materials can be cooled below the equilibrium solidus point. If the undercooling is significant, the melt freezes and forms a glass. The prediction and physical interpretation of the glass-forming ability (GFA) of undercooled melts is one of major problems in the physics of glassy materials. Quantitatively, the GFA is estimated by the critical cooling rate R_c , which is the minimal rate of melt cooling required to produce a glass. Another GFA

*Corresponding author

Email address: v.a.khonik@yandex.ru (V.A. Khonik)

measure is the maximal diameter of fully non-crystalline casting produced by melt cooling, which is called the critical diameter D_{max} . Both GFA parameters, R_c and D_{max} , are not easy to be determined and, therefore, quite a few indirect GFA measures have been proposed, which make use of a combination of characteristic temperatures, e.g. the glass transition, crystallization and liquidus temperatures [1].

The GFA of metallic glasses (MGs) has been analyzed in numerous works, e.g. see the reviews [1–3]. It is known that the GFA of metallic systems strongly depends on chemical composition so that even various minor dopants can change it strongly [4]. To interpret the GFA, different approaches are used, in particular accounting for the difference between the atomic diameters of the alloy components [5], mismatch enthalpy and entropy [6], melting and mixing enthalpy [7], mismatch entropy and configurational entropy [8], etc. [1]. However, the thermodynamic parameters used for GFA estimates [6–8] are the same for both crystalline and glassy states that strongly restricts their significance.

The entropy approach to the understanding of different MGs' properties is of a special interest [9–12]. In particular, entropy notions were recently applied to GFA analysis of MGs [2, 13]. First, it was shown that the GFA estimated via a number of parameters based on characteristic temperatures systematically increases with the excess entropy ΔS of glass with respect to the maternal crystalline state provided that this entropy is calculated for the supercooled liquid (SCL) state [2]. Therefore, the GFA of undercooled melts increases with structural disorder in the SCL state occurring upon heating. Similar conclusion was derived by the authors [13], who introduced a dimensionless parameter of structural order, $\xi(T) = 1 - \frac{\Delta S(T)}{S_m}$, where S_m is the melting entropy. A study performed on several MGs showed that ξ calculated again for the SCL state increases strongly with R_c and, therefore, the GFA increases with structural disorder controlled by the entropies ΔS and S_m . However, the use of ξ -parameter is strongly limited because the liquidus temperatures of MGs usually exceed 900 K and, therefore, it is impossible to determine the melting entropy S_m using conventional calorimeters.

In the view of the above, the aim of this work is to systematically test the hypothesis that the GFA of metallic melts is related to the excess entropy and excess enthalpy of corresponding glasses. We suggested new entropy- and enthalpy-based parameters and using the data on 26 MGs in bulk and ribbon forms showed a very good correlation of these parameters with literature data on the GFA expressed by R_c and D_{max} .

2. Experimental

Table 1 gives a list of MGs (at.%) under investigation, which were produced as either 2 mm thick plates by melt suction/jet quenching into a copper mold (labeled as bulk) or as 20–40 μm thick ribbons produced by melt spinning (labeled as ribbon). The samples were X-ray verified to be fully non-crystalline.

Differential scanning calorimetry (DSC) were performed using a Hitachi DSC 7020 instrument in 99.999 pure N_2 atmosphere on 60–70 mg samples. DSC

Table 1: Critical cooling rate R_c , critical diameter D_{max} , excess entropy ΔS and excess enthalpy ΔH of bulk and ribbon metallic glasses at the glass transition temperature T_g and in the end of the supercooled liquid range.

N	Glass	R_c [K/s]	D_{max} [mm]	ΔS_{T_g} [$\frac{J}{K \times mol}$]	ΔS_{scl} [$\frac{J}{K \times mol}$]	ΔH_{T_g} [$\frac{kJ}{mol}$]	ΔH_{scl} [$\frac{kJ}{mol}$]
1	Zr _{58.5} Nb _{2.8} Cu _{15.6} Ni _{12.8} Al _{10.3} (ribbon)	1.75 [17]	—	3.9	5.1	2.9	3.8
2	Zr ₆₆ Al ₉ Cu ₁₆ Ni ₉ (ribbon)	4.10 [3]	—	7.3	7.7	5.3	5.6
3	Zr ₆₆ Al ₈ Cu ₁₂ Ni ₁₄ (ribbon)	9.80 [3]	—	6.5	7.7	4.7	5.5
4	Zr ₅₅ Al ₁₉ Co ₁₉ Cu ₇ (ribbon)	16.0 [18]	—	3.3	3.7	2.6	2.9
5	Zr ₅₅ Al _{22.5} Co _{22.5} (ribbon)	18.0 [19]	—	7.1	7.3	5.8	6.0
6	Zr ₆₆ Al ₈ Cu ₇ Ni ₁₉ (ribbon)	22.7 [3]	—	7.5	8.3	5.4	5.9
7	Zr ₆₀ Cu ₂₀ Ni ₈ Al ₇ Hf ₃ Ti ₂ (ribbon)	33.5 [20]	—	5.2	5.7	3.7	4.1
8	Zr ₆₆ Al ₈ Ni ₂₆ (ribbon)	66.6 [3]	—	8.0	9.5	5.9	6.1
9	Zr ₆₅ Al ₁₀ Ni ₁₀ Cu ₁₅ (bulk)	4.10 [21]	—	9.0	10.4	6.6	7.5
10	Zr ₅₅ Co ₂₅ Al ₂₀ (bulk)	16.5 [18]	2.5 [22]	6.0	6.4	4.9	5.2
11	Zr ₅₇ Nb ₅ Al ₁₀ Cu _{15.4} Ni _{12.6} (bulk)	10.0 [23]	11.2 [24]	5.3	6.6	5.0	6.0
12a	Zr _{52.5} Ti ₅ Cu _{17.9} Ni _{14.6} Al ₁₀ (bulk)	4.50 [20]	10 [24]	3.8	4.4	2.8	3.2
12b	Zr _{52.5} Ti ₅ Cu _{17.9} Ni _{14.6} Al ₁₀ (bulk)	25.0 [23]	10 [24]	3.8	4.4	2.8	3.2
13	Pd ₄₀ Cu ₃₀ Ni ₁₀ P ₂₀ (bulk)	0.10 [25]	72 [24]	4.4	6.8	3.0	4.4
14	Pd ₄₀ Cu ₃₀ Ni ₁₀ P ₂₀ (ribbon)	0.10 [25]	72 [24]	3.1	4.6	2.0	3.0
15	Ti ₃₄ Zr ₁₁ Cu ₄₇ Ni ₈ (ribbon)	100 [3]	3.0 [24]	8.9	9.2	7.0	7.3
16	Zr ₅₇ Ti ₅ Al ₁₀ Cu ₂₀ Ni ₈ (ribbon)	10.0 [3]	10 [24]	4.5	4.9	3.3	3.6
17	Zr ₆₅ Al _{7.5} Cu _{17.5} Ni ₁₀ (ribbon)	1.50 [3]	16 [24]	6.2	9.6	4.5	5.6
18	Pd ₄₀ Ni ₄₀ P ₂₀ (ribbon)	1.6 [26]	25 [27]	6.3	8.4	4.2	5.5
19a	Pd ₄₀ Ni ₄₀ P ₂₀ (bulk)	1.6 [26]	25 [27]	7.5	9.8	5.1	6.4
19b	Pd ₄₀ Ni ₄₀ P ₂₀ (bulk)	0.17 [21]	25 [27]	7.5	9.8	5.1	6.4
20	Zr ₄₆ Cu ₄₆ Al ₈ (bulk)	4.0 [28]	—	3.9	5.3	3.0	4.0
21	Zr ₅₀ Cu ₅₀ (ribbon)	—	2.0 [22]	7.3	7.9	5.3	5.7
22	Zr ₄₈ Cu ₃₄ Ag ₈ Al ₈ Pd ₂ (bulk)	—	30 [29]	3.3	4.4	2.5	3.3
23	Cu ₄₉ Hf ₄₂ Al ₉ (bulk)	—	10 [27]	5.7	6.7	4.8	5.6
24	Zr ₅₀ Cu ₄₀ Al ₁₀ (bulk)	—	22 [30]	4.0	5.0	3.1	3.8
25	La ₅₅ Al ₂₅ Co ₂₀ (bulk)	—	3 [31]	8.5	9.8	4.4	5.1
26	La ₅₅ Al ₃₅ Ni ₁₀ (bulk)	—	5 [31]	7.8	8.8	4.4	4.9

measurements were performed according to the following protocol. The first heating was performed with an initial sample and an empty reference cell up to the temperature of complete crystallization T_{cr} and subsequent cooling to room temperature. This sample was next moved to the reference DSC cell. Next, a new sample of nearly the same mass was heated up to T_{cr} . This procedure allows obtaining the differential heat flow $\Delta W = W_{gl} - W_{cr}$ (W_{gl} and W_{cr} are the heat flows coming from the glass and counterpart crystal, respectively), which was further used for data analysis. The heating rate \dot{T} was 3 K/min in all cases.

The excess enthalpy ΔH and excess entropy ΔS were calculated in the way suggested recently [14, 15]:

$$\Delta H(T) = \frac{1}{\dot{T}} \int_T^{T_{cr}} \Delta W(T) dT, \quad (1)$$

$$\Delta S(T) = \frac{1}{\dot{T}} \int_T^{T_{cr}} \frac{\Delta W(T)}{T} dT. \quad (2)$$

It is seen that as temperature T approaches T_{cr} , the integrals (1) and (2) tend to zero and, therefore, ΔH and ΔS represent the excess enthalpy and entropy with respect to the crystalline state.

The relaxed state of $\text{Pd}_{40}\text{Ni}_{40}\text{P}_{20}$ glass was obtained by heating into the SCL range and subsequent cooling back at 3 K/min to room temperature.

3. Results

Figure 1(a) gives, as an example, the differential heat flow $\Delta W(T)$ for glassy ribbon $\text{Pd}_{40}\text{Ni}_{40}\text{P}_{20}$ in the initial and relaxed states, which is well-known as a good glass-former. In the initial state, small exothermal effect below the glass transition temperature T_g (which is defined as the onset of the endothermal reaction, indicated by an arrow) is determined by structural relaxation occurring upon heating. Higher temperatures belonging to the interval $T_g < T < T_x$ (T_x is crystallization onset temperature) correspond to the SCL range, which is followed by a strong exothermal crystallization ending at a temperature T_{cr} . Preliminary relaxation leads to the disappearance of the exothermal relaxation effect, as one would expect.

Panel (b) in Fig.1 shows temperature dependence of the excess enthalpy ΔH calculated using Eq.(1) with the differential heat flow $\Delta W(T)$ shown in panel (a). In the initial state, a decrease of ΔH from 4.9 kJ/mol to 3.9 kJ/mol upon heating up to T_g reflects the aforementioned exothermal structural relaxation. Entering the SCL range above T_g results in rather rapid increase of the excess enthalpy up to 4.8 kJ/mol, which is related to the endothermal heat flow in the range $T_g < T < T_x$ (panel (a)). Finally, the crystallization starting at T_x results in a rapid decrease of ΔH to zero at T_{cr} . Relaxed sample demonstrates a significantly reduced excess enthalpy below T_g but temperature dependences $\Delta H(T)$ in the initial and relaxed states at temperatures $T > T_g$ are nearly identical. Thus, heating into the SCL range removes the memory of the thermal prehistory.

All aforementioned peculiarities are further reflected in temperature evolution of the excess entropy ΔS given in Fig.1(c). Heating of an initial sample from room temperature to T_g results in a significant decrease of ΔS from 8.0 J/(mol×K) to 6.0 J/(mol×K), which demonstrates a significant structural ordering occurring upon exothermal relaxation. In the SCL region ($T_g < T < T_x$), the excess entropy rapidly increases up to $\Delta S_{scl}=7.4$ J/(mol×K) just below T_x indicating a substantial disordering of the structure. The crystallization onset at T_x leads to a rapid decrease in ΔS to zero due to the complete crystallization at T_{cr} . Preliminary relaxation leads to a significant decrease of the excess entropy

below T_g but $\Delta S(T)$ dependences at higher temperatures in the SCL range are very close.

It is further reasonable to characterize structural evolution by the disordering parameter $\alpha = \Delta S/S_m$ (S_m is the melting entropy) [16], which changes in the range $0 < \alpha < 1$. The value $\alpha \rightarrow 1$ defines a liquid-like order (close to that of a liquid) and $\alpha \rightarrow 0$ correspond to a crystal-like order. Temperature dependence of α calculated with $S_m = 14.2 \text{ J}/(\text{mol}\times\text{K})$ [13] in the initial and relaxed states are given in Fig.1(c). It is seen that, naturally, the character of temperature dependence of α repeats that of the excess entropy ΔS . Preliminary relaxation provides a substantial structural ordering below T_g . However, it should be emphasized a significant disordering described by an increase of α from 0.41 to 0.52 (that is by 27%) upon heating in the SCL range and this disordering is the same for initial and relaxed states. Nonetheless, the use of the parameter α is limited because of usually high liquidus temperatures, as mentioned above.

In this work, we are most interested in the SCL range $T_g < T < T_x$. The results described above are typical for MGs and generally indicate that this range is characterized by *i*) endothermal heat flow and corresponding rise of the excess enthalpy ΔH and *ii*) significant structural disordering reflected by an increase of the excess entropy ΔS . We show that the GFA of a *melt* can be predicted using the data on the excess entropy and excess enthalpy of the *glassy* state.

4. Discussion

We suggest that the GFA of a melt is related to the rise of the excess entropy ΔS upon heating of glass in the SCL range. This rise can be characterized by a dimensionless parameter $\sigma_{scl} = 1 - \frac{\Delta S_{T_g}}{\Delta S_{scl}}$, where the entropies ΔS_{T_g} and ΔS_{scl} are defined above (see Fig.1) and σ_{scl} indicates the strength of the disordering in the SCL range. The larger σ_{scl} , the more disorder is introduced. On the other hand, σ_{scl} characterizes the stability of supercooled liquid, i.e. the larger the σ_{scl} value, the more stable the supercooled liquid is before it crystallizes. Therefore, one can naturally consider that more stable supercooled liquid will lead to larger undercooling upon melt quenching and, respectively, to larger R_c . This idea is verified in the present work.

The entropies ΔS_{T_g} and ΔS_{scl} necessary for σ_{scl} -calculation together with literature data on R_c and D_{max} are listed in Table 1. Figure 2 shows the critical cooling rate R_c as a function of the disordering parameter σ_{scl} for MGs in bulk and ribbon forms. It is seen that $\log R_c$ steadily decreases (i.e. the GFA increases) as σ_{scl} increases, and the data scatter is quite acceptable. The best GFA among the glasses listed in Table 1 corresponds to $\text{Pd}_{40}\text{Cu}_{30}\text{Ni}_{10}\text{P}_{20}$ (lines 13,14) with $R_c \approx 0.1 \text{ K/s}$. Respectively, this glass has the largest σ_{scl} of about 0.35. The next best GFA is demonstrated by $\text{Pd}_{40}\text{Ni}_{40}\text{P}_{20}$ (lines 18,19a,19b) and $\text{Zr}_{46}\text{Cu}_{46}\text{Al}_8$. These glasses have σ_{scl} , which is a little smaller than that for $\text{Pd}_{40}\text{Cu}_{30}\text{Ni}_{10}\text{P}_{20}$.

It is also worthy of note that the data for bulk and ribbon glasses do not vary much and the corresponding linear fits are quite close. Bulk and ribbon

samples differ by orders of magnitude in the melt quenching rate upon glass production that leads to differences in their structures. However, it is known (and verified above in Fig.1) that MGs in the SCL range lose the memory of the thermal prehistory because of small relaxation time, which rapidly decreases with temperature. It is for this reason that $R_c(\sigma_{scl})$ -dependences for bulk and ribbon MGs are close to each other.

Figure 3 gives the critical diameter D_{max} as a function of σ_{scl} . Larger D_{max} corresponds to larger GFA. It is seen that $\log D_{max}$ increases with σ_{scl} . Again, the best glass-former, $\text{Pd}_{40}\text{Cu}_{30}\text{Ni}_{10}\text{P}_{20}$, which has the largest $D_{max} = 72$ mm, also has the largest $\sigma_{scl} \approx 0.35$. On the other hand, the glasses having D_{max} in the range of 1-2 mm, demonstrate the smallest σ_{scl} of about 0.03.

Thus, the data in Fig.2 and Fig.3 convincingly show that the critical cooling rate R_c and critical diameter D_{max} , which constitute direct measures of the GFA, display unambiguous dependence on structural disordering and melt stability in the SCL range given by the dimensionless parameter σ_{scl} . This conclusion agrees with a fundamental work by Li et al. [32] who fabricated over five thousand alloys and found a strong correlation between the high GFA and a direct measure of glass disorder given by the width (FWHM) of X-ray diffraction structure factor. On the other hand, the FWHM increases with temperature within the SCL range [33] providing thus direct confirmation of structural disordering in this range.

Structural disordering in the SCL region should also lead to an increase in the heat content, or the enthalpy, due to the second law of thermodynamics, $dH = TdS$ for constant pressure. One can expect, therefore, that an increase of the excess enthalpy should be proportional to the increase of the excess entropy. In this case, the rise of structural disorder and melt stability in the SCL region can be alternatively described using an enthalpy-based dimensionless parameter $\eta_{scl} = 1 - \frac{\Delta H_{T_g}}{\Delta H_{scl}}$, where the excess enthalpies ΔH_{T_g} and ΔH_{scl} correspond to the glass transition temperature T_g and the end of the SCL range (see Fig.1). These enthalpies are listed in Table 1. Figure 4 gives η_{scl} as a function of σ_{scl} . A very good linear relationship between these parameters is observed. The derivative $d\eta_{scl}/d\sigma_{scl}$ in this plot is 0.92 ± 0.01 . This means that η_{scl} is quite close to σ_{scl} and that is why it can also be used to describe the structural disordering and stability of a supercooled melt. Thus, while the parameters σ_{scl} and η_{scl} are based on qualitatively different characteristics of the SCL state, namely its structural disorder and heat content, they provide equally meaningful information about this state.

It is also important to emphasize that the σ_{scl} and η_{scl} can be determined using conventional calorimeters, as one does not need to reach usually high liquidus temperatures. It should also be pointed out that just a couple routine DSC measurements are necessary to estimate the GFA of a metallic glass.

One can suggest a qualitative interpretation of the relationship between the GFA and structural disordering in the SCL range. According to the Interstitialcy theory (IT), melting is related to a rapid multiplication of interstitial defects in the dumbbell form (called interstitialcies). These defects remain identifiable

structural units in the liquid state and melt quenching freezes a part of them in solid glass [34, 35]. Then, relaxation phenomena in MGs are determined by the changes in the defect concentration. This general approach provides quantitative interpretation of numerous relaxation effects in MGs, as described in a recent review [35].

Meanwhile, it was shown that it is the interstitial-type defect system, which almost completely determines the excess entropy ΔS and excess enthalpy ΔH of MGs with respect to their counterpart crystals [15, 35]. Indeed, ΔH simply constitutes the elastic energy of the defect system accurate to a precision of 10–15% [15]. On the other hand, the excess enthalpy ΔH is proportional to the excess entropy ΔS of glass [36] (this also follows from Fig.4) and, therefore, the latter is determined by glass defect structure as well.

Interstitial-type defects increase the vibrational entropy of glass through their strong low-frequency vibrational modes [34, 35]. Structural disordering due to increasing defect concentration leads to a rise of the vibrational component of the entropy. Thus, the total excess entropy of glass ΔS increases with the defect concentration while the latter increases with temperature in the SCL range [35, 37]. This should result in an increase of ΔS and ΔH in the SCL range, as indeed observed (see Fig.1).

On the other hand, an increase of the defect concentration in the SCL range leads to simultaneous increase of structural disorder given by the width (FWHM) of X-ray structure factor [37]. Since the increase of the normalized FWHM with temperature approximately equals to the rise of the defect concentration [37], one should accept that structural disordering in the SCL range quantified by an increase of the FWHM and σ_{scl} is mainly caused by an increase in the defect concentration. Consequently, given that σ_{scl} also reflects the structural stability in the SCL range, one can expect that the GFA of *undercooled melt* is governed by the defect concentration in the SCL state of *glass* as well. This is an intriguing direction for further research since it provides a completely new window to the understanding of the GFA of metallic glasses.

5. Conclusions

We performed differential scanning calorimetry on 26 metallic glasses in bulk and ribbon forms. On this basis, temperature dependences of the excess entropy and excess enthalpy of these glasses with respect to their counterpart crystals are calculated. Using the excess entropy, we introduced a dimensionless parameter σ_{scl} , which characterizes the structural disordering and structural stability of the supercooled liquid (SCL) state. It is found that σ_{scl} strongly correlates with the critical cooling rate R_c and critical diameter D_{max} , which can be achieved upon glass production. Alternatively, we introduced a dimensionless parameter η_{scl} based on the excess enthalpy in the supercooled liquid state, which equally good correlates with R_c and D_{max} .

Our investigation provides convincing arguments that glass-forming ability (GFA) of a melt characterized by R_c and D_{max} is intrinsically related to the degree of structural disorder, structural stability and heat content achieved upon

heating above the glass transition temperature before the crystallization takes place. Possible relationship of these findings with the defect structure of metallic glasses is discussed. It is argued that the GFA of an undercooled melt is related to the defect concentration in the SCL state of glass.

The parameters σ_{scl} and η_{scl} introduced in this work are very convenient for an express estimate of the GFA.

6. Author Contributions

J.B.C. and G.J.L. contributed to the preparation of samples, R.A.K., A.S.M. and G.V.A. performed DSC measurements and data analysis, J.C.Q., N.P.K. and V.A.K. prepared and edited the manuscript, V.A.K. conceived the idea and supervised the project.

7. Acknowledgments

The work was supported by Russian Science Foundation under the project 23-12-00162.

References

- [1] C. Chattopadhyay, K.S.N. Satish Idury, J. Bhatt, K. Mondal, B.S. Murty, Critical evaluation of glass forming ability criteria, *Mater. Sci. Technol.* 32 (2016) 380-400.
- [2] A. S. Makarov, R.A. Konchakov, G.V. Afonin, J.C. Qiao, N.P. Kobelev, V.A. Khonik, Excess entropy of metallic glasses and its relation to the glass-forming ability of maternal melts, *J. Exp. Theor. Pys. Lett.* 120 (2024) 759–765.
- [3] Z.P. Lu, H. Bei, C.T. Liu, Recent progress in quantifying glass-forming ability of bulk metallic glasses, *Intermetallics* 15 (2007) 618-624.
- [4] Wang, W. H. Roles of minor additions in formation and properties of bulk metallic glasses, *Prog. Mater. Sci.* 52 (2007) 540-596.
- [5] A. Inoue, Stabilization of metallic supercooled liquid and bulk amorphous alloys, *Acta Mater.* 48 (2000) 279-306.
- [6] A. Takeuchi, A. Inoue, Calculations of mixing enthalpy and mismatch entropy for ternary amorphous alloys, *Mater. Trans. JIM* 41 (2000) 1372-1378.
- [7] A.-H. Cai, H. Chen, W.-K. An, J.-Y. Tan, Y. Zhou, Relationship between melting enthalpy H_m and critical cooling rate R_c for bulk metallic glasses, *Mater. Sci. Eng. A* 457 (2007) 6–12.

- [8] B.R. Rao, M. Srinivas, A.K. Shah, A.S. Gandhi, B.S. Murty, A new thermodynamic parameter to predict glass forming ability in iron based multi-component systems containing zirconium, *Intermetallics* 35 (2013) 73-81.
- [9] G.P. Johari, Source of JG-relaxation in the entropy of glass, *J. Phys. Chem. B* 123 (2019) 3010-3023.
- [10] X. Feng, Y. Yue, J. Qiu, H. Jain, S. Zhou, Entropy engineering in inorganic non-metallic glass, *Fund. Research* 2 (2022) 783-793.
- [11] X. Lu, S. Feng, L. Li, L.M. Wang, R. Liu, Depicting defects in metallic glasses by atomic vibrational entropy, *J. Phys. Chem. Lett.* 14 (2023) 6998-7006.
- [12] M. Yang, W. Li, X. Liu, H. Wang, Y. Wu, X. Wang, F. Zhang, Q. Zeng, D. Ma, H. Ruan, Z. Lu, Configurational entropy effects on glass transition in metallic glasses, *J. Phys. Chem. Lett.* 13 (2022) 7889-7897.
- [13] A.S. Makarov, G.V. Afonin, R.A. Konchakov, V.A. Khonik, J.C. Qiao, A.N. Vasiliev, N.P. Kobelev, Dimensionless parameter of structural ordering and excess entropy of metallic and tellurite glasses, *Scr. Mater.* 239 (2024) 115783.
- [14] A.S. Makarov, G.V. Afonin, J.C. Qiao, A.M. Glezer, N.P. Kobelev, V.A. Khonik, Determination of the thermodynamic potentials of metallic glasses and their relation to the defect structure, *J. Phys.: Condens. Matter* 33 (2021) 435701.
- [15] A.S. Makarov, M.A. Kretova, G.V. Afonin, J.C. Qiao, A.M. Glezer, N.P. Kobelev, V.A. Khonik, On the nature of the excess internal energy and entropy of metallic glasses, *J. Exp. Theor. Phys Lett.* 115 (2022) 102-107.
- [16] G.V. Afonin, A.S. Makarov, R.A. Konchakov, J.C. Qiao, A.N. Vasiliev, N.P. Kobelev, V. Khonik, Thermodynamic entropy-based parameter of structural disordering and its relation to the width of the X-ray structure factor and defect concentration in a metallic glass, *J. Alloys Compd.* 983 (2024) 173836.
- [17] C.C. Hays, J. Schroers, W.L. Johnson, T.J. Rathz, R.W. Hyers, J.R. Rogers, M.B. Robinson, Vitrification and determination of the crystallization time scales of the bulk-metallic-glass-forming liquid $Zr_{58.5}Nb_{2.8}Cu_{15.6}Ni_{12.8}Al_{10.3}$, *Appl. Phys. Lett.* 79 (2001) 1605-1607.
- [18] S. Mukherjee, H.-G. Kang, W.L. Johnson, and W.-K. Rhim, Noncontact measurement of crystallization behavior, specific volume, and viscosity of bulk glass-forming Zr-Al-Co-(Cu) alloys, *Phys. Rev. B* 79 (2004) 174205.
- [19] S. Mukherjee, J. Schroers, W.L. Johnson, W.-K. Rhim, Influence of kinetic and thermodynamic factors on the glass-forming ability of zirconium-based bulk amorphous alloys, *Phys. Rev. Lett.* 94 (2005) 245501.

- [20] D. Xing, J. Sun, G. Wang, and M. Yan, The relations between ΔT_x and the glass forming ability of bulk amorphous Zr–Cu–Ni–Al–Hf–Ti and Zr_{52.5}Cu_{17.9}Ni_{14.6}Al₁₀Ti₅ alloys, *J. Alloys Compd.* 375 (2004) 239-242.
- [21] W.H. Wang, Correlations between elastic moduli and properties in bulk metallic glasses, *J. Appl. Phys.* 99 (2006) 093506.
- [22] Z. Long, H. Wei, Y. Ding, P. Zhang, G. Xie, A. Inoue, A new criterion for predicting the glass-forming ability of bulk metallic glasses, *J. Alloys Compd.* 475 (2009) 207–219.
- [23] C. W. Ryu, D.H. Kang, S. Jeon, G.W. Lee, E.S. Park, Accurate quantification of glass-forming ability by measuring effective volume relaxation of supercooled melt, *APL Mater.* 5 (2017) 106103.
- [24] C. Chattopadhyay, K.S.N. Satish Idury, J. Bhatt, K. Mondal, B.S. Murty, Critical evaluation of glass forming ability criteria, *Mater. Sci. Technol.* 32 (2016) 380-400.
- [25] A. Inoue, N. Nishiyama, H. Kimura, Preparation and thermal stability of bulk amorphous Pd₄₀Cu₃₀Ni₁₀P₂₀ alloy cylinder of 72 mm in diameter, *Mater. Trans.* 38 (1997) 179-183.
- [26] O.N. Senkov, Correlation between fragility and glass-forming ability of metallic alloys, *Phys. Rev. B* 76 (2007) 104202.
- [27] Y.-C. Hu, J. Schroers, M.D. Shattuck, C.S. O’Hern, Tuning the glass-forming ability of metallic glasses through energetic frustration, *Phys. Rev. Mater.* 3 (2019) 085602.
- [28] S. Lan, X. Wei, J. Zhou, Z. Lu, X. Wu, M. Feygenson, J. Neuefeind, X.-L. Wang, In-situ study of crystallization kinetics in ternary bulk metallic glass alloys with different glass forming abilities, *Appl. Phys. Lett.* 105 (2014) 201906.
- [29] R. Deng, Z. Long, L. Peng, D. Kuang, B. Ren, A new mathematical expression for the relation between characteristic temperature and glass-forming ability of metallic glasses, *J. Non-Cryst. Sol.* 533 (2020) 119829.
- [30] A. Inoue, A. Takeuchi, Recent development and application products of bulk glassy alloys, *Acta Mater.* 59 (2011) 2243–2267.
- [31] A. Ghorbani, A. Askari, M. Malekan, M. Nili-Ahmadabadi, Thermodynamically-guided machine learning modelling for predicting the glass-forming ability of bulk metallic glasses. *Sci. Rep.* 12 (2022) 11754.
- [32] M.-X. Li, Y.-T. Sun, C. Wang, L.-W. Hu, S. Sohn, J. Schroers, W.-H. Wang, Y.-H. Liu, Data-driven discovery of a universal indicator for metallic glass forming ability, *Nature Mater.* 21 (2022) 165-171.

- [33] N. Neuber, O. Gross, M. Frey, B. Bochtler, A. Kuball, S. Hechler, I. Gallino, R. Busch, On the thermodynamics and its connection to structure in the Pt-Pd-Cu-Ni-P bulk metallic glass forming system, *Acta Mater.* 220 (2021) 117300.
- [34] A.V. Granato, Interstitialcy theory of simple condensed matter, *Eur. J. Phys. B* 87 (2014) 18.
- [35] N.P. Kobelev, V.A. Khonik, A novel view of the nature of formation of metallic glasses, their structural relaxation, and crystallization, *Physics–Uspekhi* 66 (2023) 673-690.
- [36] G.V. Afonin, J.C. Qiao, A.S. Makarov, R.A. Konchakov, E.V. Goncharova, N.P. Kobelev, V.A. Khonik, High entropy metallic glasses, what does it mean? *Appl. Phys. Lett.* 124 (2024) 151905.
- [37] A.S. Makarov, G.V. Afonin, R.A. Konchakov, J.C. Qiao, A.N. Vasiliev, N.P. Kobelev, V.A. Khonik, Defect-induced ordering and disordering in metallic glasses, *Intermetallics* 163 (2023) 108041.

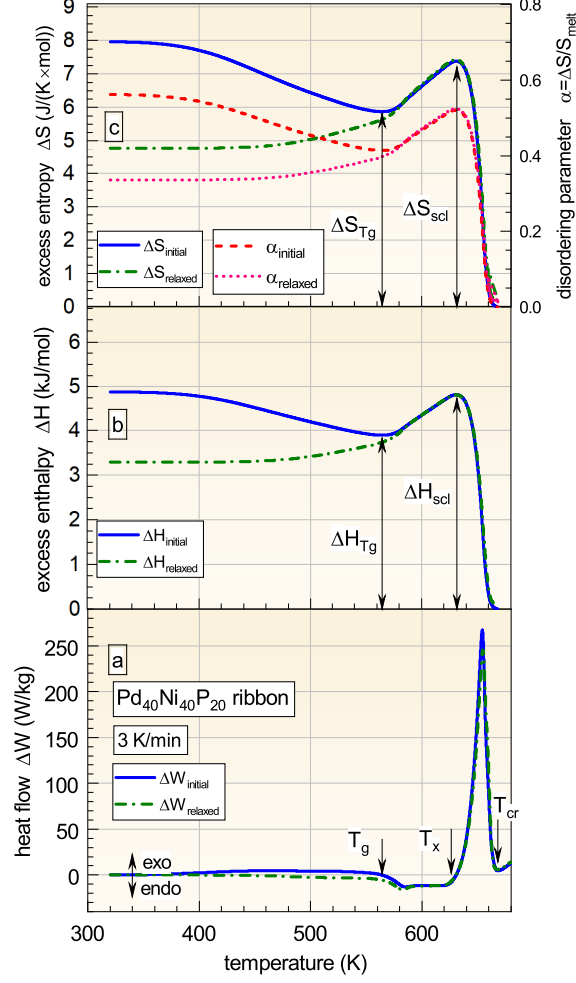


Figure 1: Differential heat flow ΔW (a), excess enthalpy ΔH (calculated with Eq.(1)) (b), excess entropy ΔS (calculated with Eq.(2)) and disordering parameter $\alpha = \Delta S/S_m$ (c) for glassy ribbon $\text{Pd}_{40}\text{Ni}_{40}\text{P}_{20}$ in the initial and relaxed states as functions of temperature. The characteristic temperatures – glass transition T_g , crystallization onset T_x and complete crystallization T_{cr} , are indicated. The enthalpy ΔH_{Tg} and entropy ΔS_{Tg} at $T = T_g$ together with the enthalpy ΔH_{scl} and entropy ΔS_{scl} corresponding to the end of the SCL range are also shown.

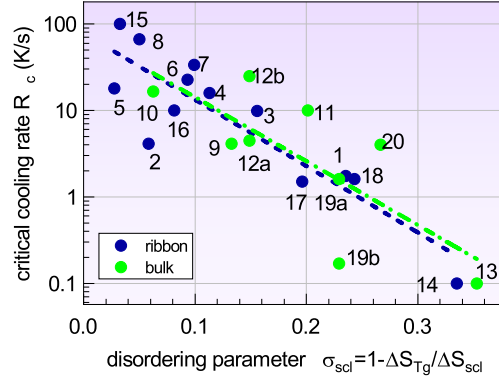


Figure 2: Critical cooling rate R_c as a function of the disordering parameter σ_{scl} for ribbon and bulk glasses. The numbers indicate MGs' compositions according to Table 1. The lines give least square fits. The Pearson correlation coefficient is 0.86 and 0.89 for bulk and ribbon glasses, respectively.

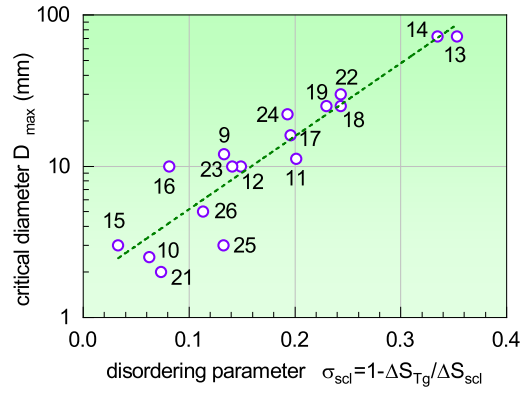


Figure 3: Critical diameter D_{max} as a function of the disordering parameter σ_{scl} for bulk glasses. The line gives the least square fit with a Pearson correlation coefficient of 0.94.

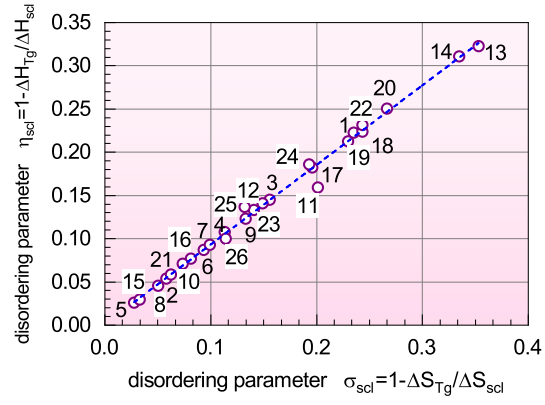


Figure 4: Relationship between the enthalpy-based η_{scl} and entropy-based σ_{scl} parameters of structural disorder and stability in the supercooled liquid range. The slope $d\eta_{scl}/d\sigma_{scl} = 0.92 \pm 0.01$.